Supporting Information

Self-assembly of Chimeric Peptides Toward Molecularly Defined Hexamers with Controlled Multivalent Ligand Presentation

Xiushuang Yuan[‖],[1,2] Linhai Jiang[‖],[3] Weike Chen,[2] Bo Song,[4] Wei Chen,[5] Xiaobing Zuo,[6] Xiankai Sun,[7] Xiaopeng Li,[4] Kent Kirshenbaum,[3] Shizhong Luo,[1] He Dong[2]*

1. College of Life Science and Technology, Beijing University of Chemical Technology, North 3rd Ring Rd 15, Chaoyang District, Beijing, 10002 (China)
2. Department of Chemistry and Biochemistry, The University of Texas at Arlington, 701 S Nedderman Drive, Arlington, TX 76019 (USA)
3. Department of Chemistry, New York University, 100 Washington Square East, New York, NY, 10003 (USA)
4. Department of Chemistry, The University of South Florida, 4202 E Fowler Avenue, Tampa, FL, 33620 (USA)
5. Department of Physics, The University of Texas at Arlington, 701 S Nedderman Drive, Arlington, TX 76019 (USA)
6. X-ray Science Division, Argonne National Laboratory, 9700 South Cass Avenue, Lemont, IL 60439 (USA)
7. Department of Radiology, The University of Texas Southwestern Medical Center, 5323 Harry Hines Boulevard, Dallas, TX 75390 (USA)

E-mail: he.dong@uta.edu

Materials

Fmoc protected amino acid, MBHA rink amide resin and 2-(1H-benzotriazol-1-yl)-1,1,3,3-tetramethyluronium hexafluorophosphate (HBTU) were purchased from Novabiochem. 5(6)-Carboxyfluorescein (FAM), N, N-Diisopropylethylamine (DIPEA), acetic anhydride, triisopropylsilane (TIS), piperidine, 1,2-ethanedithiol (EDT), 2,2'-dithiodipyridine, and methylthiazolyldiphenyl-tetrazolium bromide (MTT) assay kit were purchased from Sigma. N, N-dimethylformamide (DMF), acetic anhydride, trifluoroacetic acid (TFA), diethyl ether, dithiothreitol (DTT), methanol, Tris buffer (1 M, pH=7.5), monosodium phosphate, disodium phosphate and glycine were purchased from Fisher Scientific. U87 MG cell line was provided by Dr. Xiankai Sun lab at UT Southwestern Medical Center.[1] NIH/3T3 mouse fibroblast cell line was provided by Dr. Liping Tang lab at the University of Texas at Arlington. Eagle's Minimum Essential Medium (EMEM) was purchased from ATCC. Fetal bovine serum was purchased from VWR. All materials were used as received.

Methods

1. Synthesis and purification of peptides

All peptides were synthesized on a *Prelude*® peptide synthesizer using standard Fmoc-solid phase peptide synthesis at a scale of 50 μmole. 20% (V/V) piperidine was used to deprotect the Fmoc group followed by amino acid coupling using HBTU and DIPEA as coupling reagents in a molar ratio of 1:1:2 (amino acid: HBTU: DIPEA). Fmoc protected amino acids were added in 4 equivalents of MBHA rink amide resin. The N-terminus was acetylated in the presence of acetic anhydride and DIPEA in DMF. Peptides were cleaved from resins in a mixture of TFA/ TIS/ water/ EDT (91/ 3/ 3/ 3 by volume with a total of 5 mL) for 3 hours. TFA solution was collected and the resin was rinsed twice with neat TFA. After TFA evaporation, the residual peptide solution was triturated with cold diethyl ether. The resulting precipitate was centrifuged and washed 3 times by cold diethyl ether. Crude peptides were dried under vacuum overnight for purification by reverse phase HPLC using a binary mobile phase composed of water and acetonitrile in the presence of 0.05% TFA. Elution was monitored at 230 nm and 280 nm.

Fluorescein terminated peptides were synthesized as follows. After final deprotection, the N-terminus was coupled with 4 equivalents of 5(6)-carboxyl fluorescein using a

combination of 4 equivalents of HBTU and 8 equivalents of DIPEA in DMF. The reaction mixture was stirred overnight. The completion of the coupling reaction was confirmed by the Kaiser test. If necessary, the coupling of 5-(6)-carboxyl-fluorescein was repeated one more time. The cleavage and purification procedure followed the same procedure as described for the nonlabelled peptides.

To synthesize chimeric peptide conjugates, the cysteine residue on P7 or P6 was activated with 2,2'-dithiodipyridine. 10 mL of P7 or P6 solution (1 mg/mL in 20 mM Tris buffer, pH=7.4) was mixed with 2 mL of 2,2'-dithiodipyridine (5 mg/ mL in methanol solution). The reaction was kept at room temperature for overnight followed by extraction with diethyl ether to remove excessive 2,2'-dithiodipyridine. The aqueous layer containing activated P7 or P6 was purified on HPLC and lyophilized. P7-26r or P6-26r conjugates were synthesized by mixing 5 mL of activated P7 or P6 solution (1 mg/mL in 20mM Tris buffer, pH=7.4) and 5 mL of 26r solution (1 mg/mL in 20mM Tris buffer, pH=7.4). The mixture was stirred for overnight followed by purification on HPLC. The molecular weight of each peptide was determined by MALDI-TOF mass spectrometry using α-cyano-4-hydroxycinnamic acid as the matrix. The results are shown in **Table S1** and the mass spectra of the conjugates are shown in **Fig. S1**.

Table S1. List of peptides used in the study and expected and observed mass

	Expected mass ($[M+H]^+$ or $[M+Na]^+$)	Observed mass ($[M+H]^+$ or $[M+Na]^+$)
26r	2984.5	2984.1
26r (P)	2872.2	2872.5
FITC-26r	3436.6	3436.8
FITC-26r(P)	3302.3	3303.4
P6	1943.1	1943.0
P7	2210.4	2210.5
RGDS-P7sr	2990.3	2988.2
RGDS-P7	2721.9	2721.8
P6-26r	4902.6	4902.4
P7-26r	5169.9	5167.6

(RGDS-P7)-26r	5682.3	5683.3
P7-(FITC-26r)	5600.9	5601.8
(RGDS-P7)-(FITC-26r)	6134.4	6136.3
(RGDS-P7)-(FITC-26r(P))	6001.2	6001.0
(RGDS-P7sr)-(FITC-26r)	6380.1	6380.7
(DGSR-P7)-(FITC-26r)	6134.4	6136.9

2. Circular Dichroism (CD) Spectroscopy

Peptide samples were prepared by dissolving lyophilized peptide powders in phosphate buffer (10 mM, pH 7.4) to reach a concentration at ~ 1 mM as the stock solution. The stock solution was diluted in the same phosphate buffer to reach a concentration at 100 μM. The diluted peptide solution was annealed at 70 ℃ for 10 mins and incubated at 4 ℃ for overnight before measurements. Data were collected between 250 nm and 190 nm at room temperature with a scanning rate at 100 nm/min, a response time of 2 sec and a bandwidth of 1 nm. For melting curve measurements, spectra were acquired by monitoring the ellipticity at 225 nm while heating peptide solution from 5 ℃ to 95 ℃ with a heating rate of 20 ℃/hr. The raw data of melting curve was fitted by the sigmoidal Boltzmann equation implemented in OriginPro 8.5.

3. Small Angle X-Ray Scattering (SAXS)

Samples for SAXS measurements were prepared by direct dissolution of peptide powders in 10 mM sodium phosphate buffer (pH=7.4) to reach a concentration in the range of 500 μM to 600 μM. SAXS experiments were performed at beamline 12-ID-B of the Advanced Photon Source, Argonne National Laboratory. Scattering data were obtained using an x-ray radiation of 14.0 keV and a detector distance of 2.0 m covering a Q-range ($Q=4\pi\sin(\theta/2)/\lambda$, λ is the x-ray wavelength, θ is the scattering angle) of ~ 0.004 - 0.9 $Å^{-1}$. Mw of P7-26r assembly was calculated through extrapolation to Q -> 0 using a Guinier analysis by following Equation (1) using water as absolute scattering standard and the forward scattering intensity, I(Q=0), obtained from the Guinier analysis.[2]

$$M_w = \frac{N_0 \times I_0}{c(\rho_M - \rho_S)^2}$$

Equation (1)

where M_w is protein molecular weight in kDa, N_0 is Avogadro's constant, I_0 is forward scattering intensity in cm^{-1}, c is protein concentration in mg/ml, and $(\rho_M-\rho_S)$ is scattering length density difference (2.086×10^{10} cm^{-2}). The molecular weight of P7-26r determined in this method was ~33 kDa. (**Fig. 2A**)

A different method was also employed for determining the molecular weight of P7-26r from SAXS data as described below. Convergence of QI(Q) versus Q plot (**Figure S3**) allowed the application of a concentration, shape-independent and standard-free method to estimate the M_w of the assembly via Equation (2).[3]

$$M_w = \left(\frac{\left(\frac{I_0}{0.25\ \text{Å}^{-1}}\right)^2}{e^c \times R_g}\right)^{1/k} \int_0 QI(Q)dQ$$

Equation (2)

where M_w is protein molecular weight in Da, I_0 is forward scattering intensity in cm^{-1}, Q is scattering vector in $Å^{-1}$, I(Q) is scattering intensity in cm^{-1}, R_g is radius of gyration in Å, e is Euler's number, k (1.0) and c (-2.0948) are protein-specific empirical parameters. The Mw of P7-26r determined in this way was ~32 kDa, consistent with the result from the previous method.

4. Electrospray ionization mass spectrometry (ESI-MS)

ESI-MS was conducted on a Waters Synapt G2 mass spectrometer. All samples were diluted using deionized water to a concentration of 50 μM and were incubated at 4 °C for overnight before being injected into the ESI probe using direct infusion at a flow rate of 3 mL/h. The instrument was set under the following conditions: ESI capillary voltage, 2.0-3.0 kV; sample cone voltage,10 V; extraction cone voltage, 0.1 V; source temperature 100 ºC; desolvation temperature, 170 ºC; cone gas flow, 10 L/h; desolvation gas flow, 700 L/h (N_2); source gas control, 0 mL/min; trap gas control, 2.5 mL/min.

5. Cell uptake assay

U87MG or NIH/3T3 mouse fibroblast cell suspensions were seeded in a confocal dish. After 24 hours of incubation, the dish was washed with PBS buffer for three times to remove any non-adherent cells. FITC-labeled chimeric peptides were diluted to a concentration of 500 μM and subject to annealing as described for samples used for CD measurement.180 μL of EMEM cell culture media and 20 μL of peptides were added to the confocal dish to reach a final peptide concentration at 50 μM. After 24 hours of incubation, cells were washed with PBS buffer for three times to remove any non-specific bound peptides. Cells were stained with nuclear-specific dye, Hoechst 33342 at room temperature for 15 min and washed with PBS buffer for three times. Images were captured using a fluorescence microscope and processed with ImageJ software.

6. MTT assay

U87MG cells were seeded in a 96-well plate at a density of 10^4 cells/well and incubated at 37 °C in an incubator with 5% of CO_2. After 24 hours, culture media were removed. 10 μL of peptide solution in PB buffer (pH 7.4, 10mM) at various concentrations (1000, 500, 200 μM) was mixed with 90 μL cell culture medium in a 96-well plate. After 24 hours of incubation, MTT assay was performed to quantify the cell viability by monitoring the UV absorbance at 570 nm. Cells without peptides were used as a control. All the experiments were performed in four replicates.

7. Analytical Ultracentrifugation

Sedimentation velocity experiments were performed with a Beckman-Coulter Optima XL-I analytical ultracentrifuge equipped with an An-50 Ti 8-hole rotor. Double-sector centerpieces sandwiched between sapphire windows in a standard cell housing were loaded with 400 μL of sample and an equal volume of reference buffer (10 mM PB buffer, pH=7.4). The samples were prepared the same as those for CD measurements. After 2-hour equilibration under vacuum, samples were centrifuged at 50,000 rpm at 20 deg. C. Data were acquired using absorbance optics tuned to 280 nm for each sample reading. Sedimentation velocity data were fitted to a continuous *c(s)* distribution model using SEDFIT software.[4] The buffer density and

viscosity at room temperature were determined to be 0.99914 g/mL and 0.01005 cP, respectively using SEDNTERP.[5] The partial-specific volume of P7-26r was estimated to be 0.73317 mL/g and that of (RGDS-P7)-26r was 0.72508 mL/g. A resolution of 100 was used, and a regularization level of 0.95 was employed. Time-invariant noise elements were removed from the data.[6] All figures featuring *c(s)* distributions were generated in GUSSI software.[7]

8. Molecular Dynamic (MD) Simulation

Construction of the P7-26r hexamer

The initial conformation of 26r coiled coil dimer was built by using CCBuilder 2.0[8] and that of P7 collagen triple helices was modified from the crystal structure of $[(\text{Pro-Pro-Gly})_{10}]_3$ (pdb code: 1K6F)[9]. The sequence (in the heptad pattern, Ile at *a*, Leu at *d*, Lys at *e* and Glu at *g* positions, respectively) of 26r features parallel and dimeric coiled coil topology.[10] The dimeric oligomerization state of 26r has been verified by small angle X-ray scattering in our previous work.[11] An in-house python script (available upon request) was used to assemble three coiled coils and two collagen triple helices together to reproduce the experimental SAXS profiles. The general procedure of the construction is as follows:

1. In the Cartesian coordinate system, three coiled coils were initially placed at such locations that their symmetry-axis are on the x-y plane. The angle between the symmetry-axis of any two coiled coils was set as 120°C and this value was kept unchanged during the rigid body transformation. The three symmetry-axis all pass through the origin point. All N-termini are placed facing toward the origin point.
2. The two collagen triple helices were placed with their symmetry-axes on the z-axis and the N-termini facing toward the origin point.
3. During the virtual conjugation process, the following parameters are adjusted: (**a**) the distance from the geometric center of collagen triple helices to the x-y plane, (**b**) the distance between the symmetry-axis of the collagen triple helices and the z-axis, (**c**) the distance from the origin point to the symmetry-axis of the coiled coil, (**d**) the side chain dihedral angle of cysteine residues in both coiled coils and collagen triple helices, (**e**) the backbone phi and psi angles of PCGP segments in the collagen triple helices and (**f**)

both coiled coils and collagen triple helices are allowed to rotate around their symmetry-axes.

4. The parameters specified in step (3) were altered in an iterative fashion until the distances between paired sulfur atoms were in the range of 2.0-2.1Å. Steric clash was avoided for each search step.

Simulation details

All computational works were carried out using Prince high performance computing clusters in New York University. The PMEMD.MPI module of Amber18 was used for energy minimizations and PMEMD. Cuda module of Amber18 was used for equilibrium and production runs.[12] Amber force field ff14SB[13] was used to model the peptides, tip3p[14] water model was selected as the solvent molecule and sodium ions[15] was used only for charge neutralization. For mimicking the experimental buffer condition, no additional sodium or chloride ions were added. The buffer distance between the peptides and simulation box boundary was set as 12 Å. The SHAKE algorithm[16] was used to constrain bonds involving hydrogen atoms. Force evaluation was set with a 12 Å cutoff for Lennard-Jones interactions and a 9 Å cutoff for electrostatic interactions (calculated by smooth PME electrostatics[17]) in a periodic boundary condition. The simulation temperature was controlled with a Langevin thermostat[18] with a collision frequency of 1 ps^{-1}. For NPT runs, constant pressure (1bar) was controlled by a Berendsen barostat[19] with isotropic pressure scaling. Water molecules and peptide residues whose dihedral angles had been randomized during the initial structure construction step were relaxed by 100 steps of steep-descent minimization and 900 steps of conjugate gradient minimization with a restraint of 256 kcal/mol-$Å^2$ applied to the other residues. The entire simulation system was relaxed in the same manner but without any restraint. A 50-ps run in constant volume was performed to gradually increase the temperature from 0.1 K to 298 K with 256 kcal/mol-$Å^2$ applied to the **P7-26r** hexamer at a 1fs time step, followed by another 252-ps NVT run with restraint gradually reduced to 4 kcal/mol-$Å^2$ at a 1.5 fs time step. The restraint was gradually released over the following 400-ps NPT run using a 2-fs time step. The production run was propagated in NPT ensemble for 1000 ns with no restraint. All data analysis was done by using Cpptraj package implemented in Amber18 suite.[20]

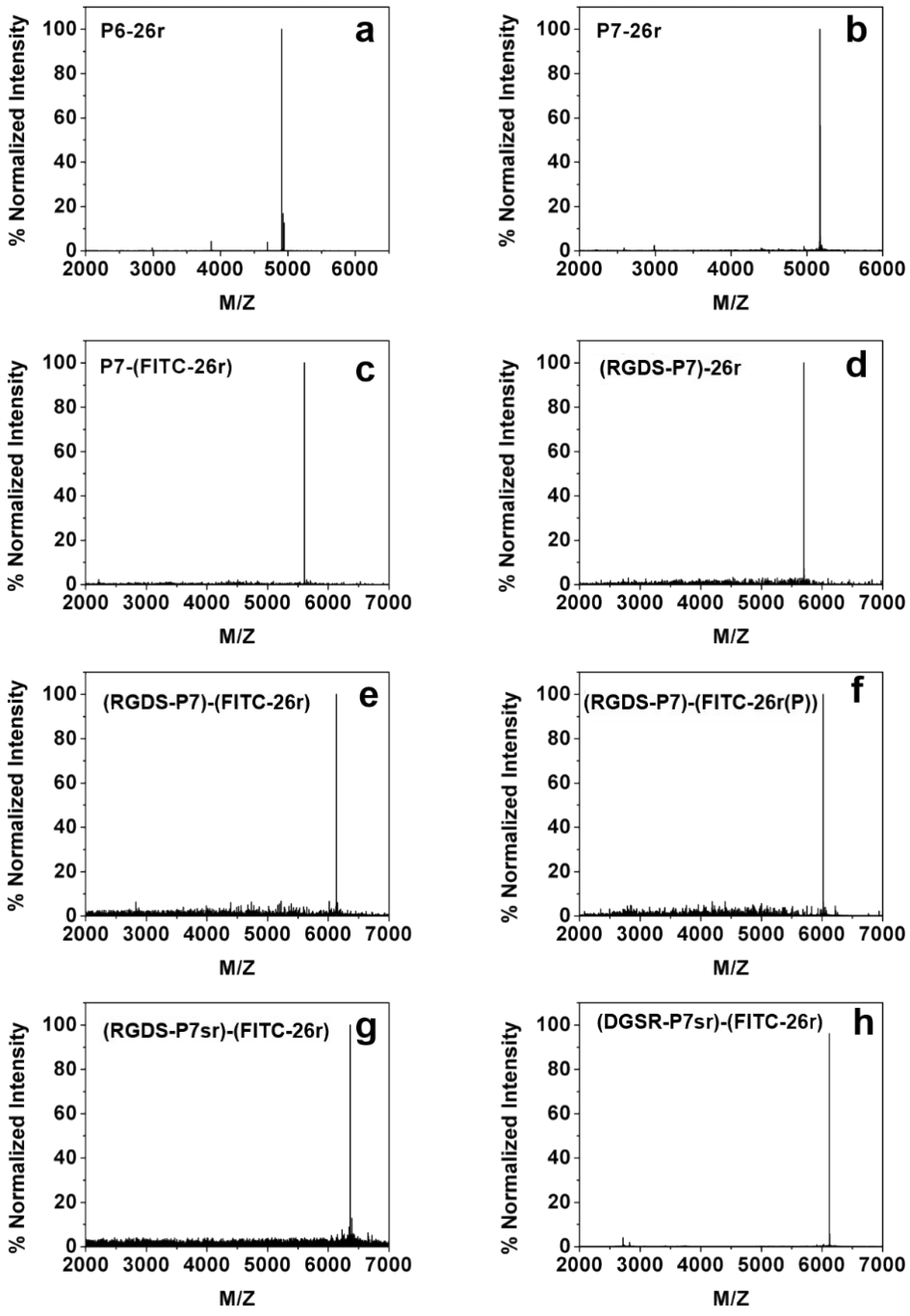

Figure S1. MALDI spectra of (**a**) P6-26r (**b**) P7-26r (**c**) P7-(FITC-26r) (**d**) (RGDS-P7)-26r (**e**) (RGDS-P7)-(FITC-26r) (**f**) (RGDS-P7)-(FITC-26(P)), (**g**) (RGDS-P7sr)-(FITC-26r), (h) (DGSR-P7)-(FITC-26r).

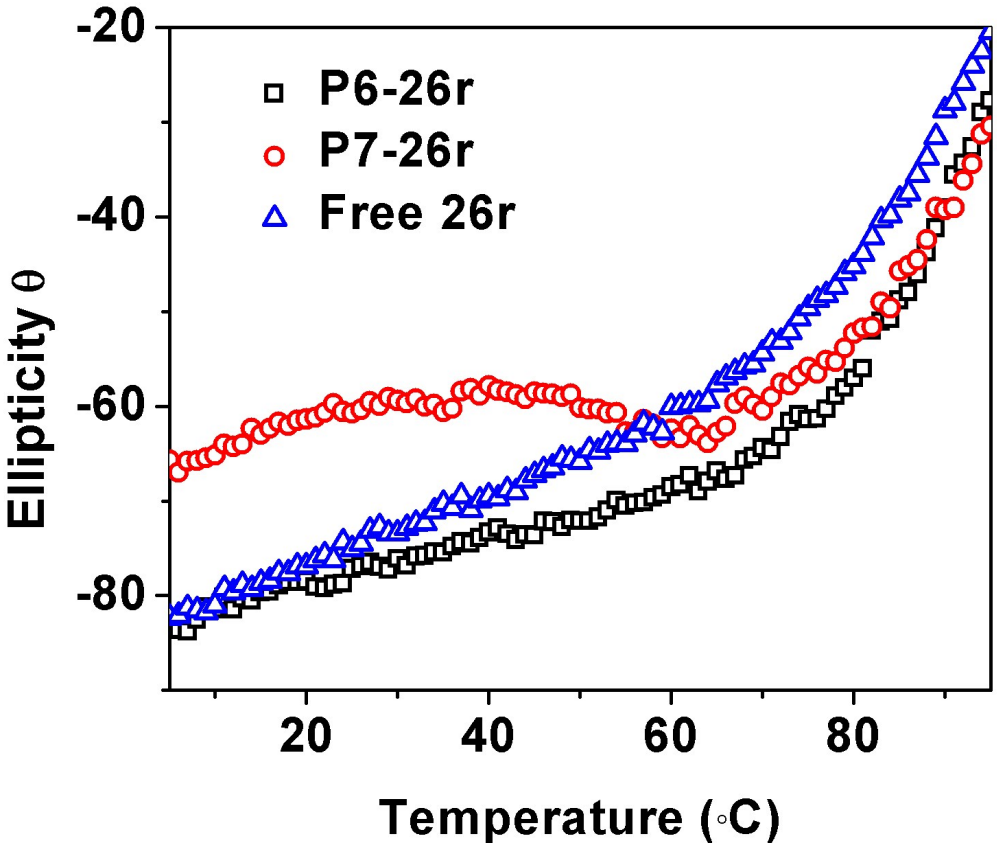

Figure S2. Thermal unfolding profiles of free 26r, P6-26r and P7-26r assemblies by monitoring the ellipticity at 225 nm. Peptide concentration: 100 μM. Buffer: 10 mM sodium phosphate buffer (pH=7.4)

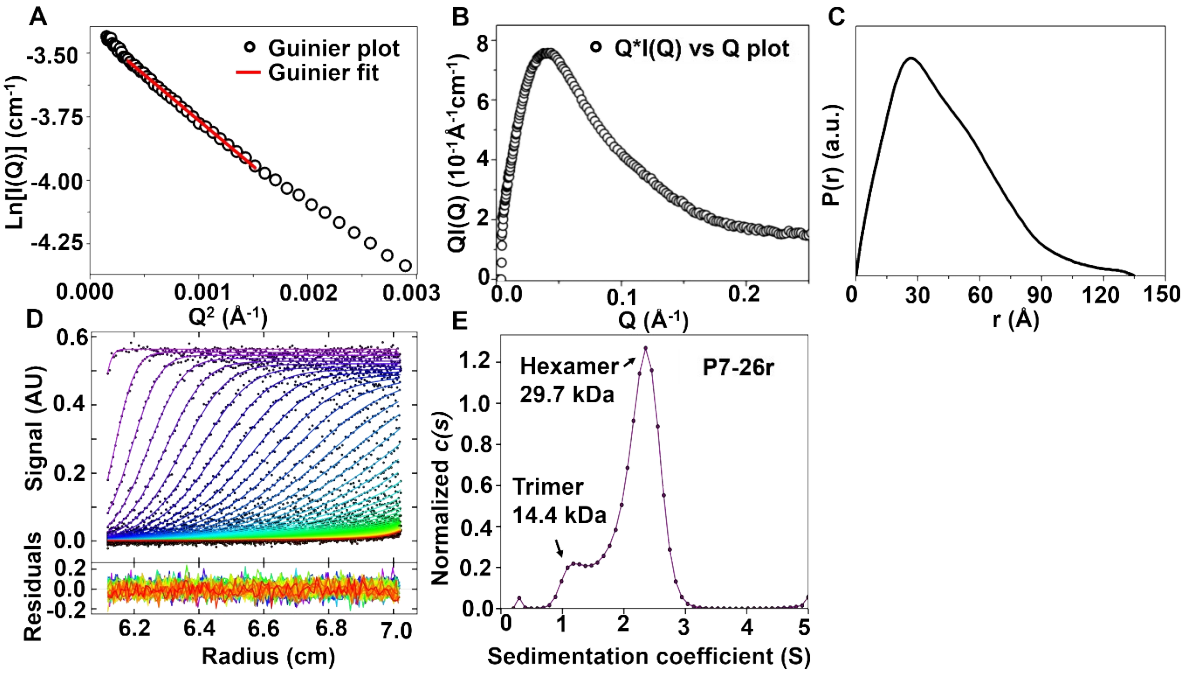

Figure S3. (A) Guinier plot of P7-26r assembly in low scattering vector Q region. (B) QI versus Q plot of P7-26r assembly for Mw estimation. The Mw was determined to be ~32 kDa, corresponding to six subunits. (C) The P(r) function computed from the SAXS data with the GNOM program. (D) Raw sedimentation profiles of absorbance at 280 nm versus cell radius (top trace) and residual plot supplied by SEDFIT software (bottom trace). (E) Continuous sedimentation coefficient distribution, c(s) curve showing predominance of hexamers mixed with small amounts of trimers. Peptide concentration is 500 µM for SAXS and 100 µM AUC analysis.

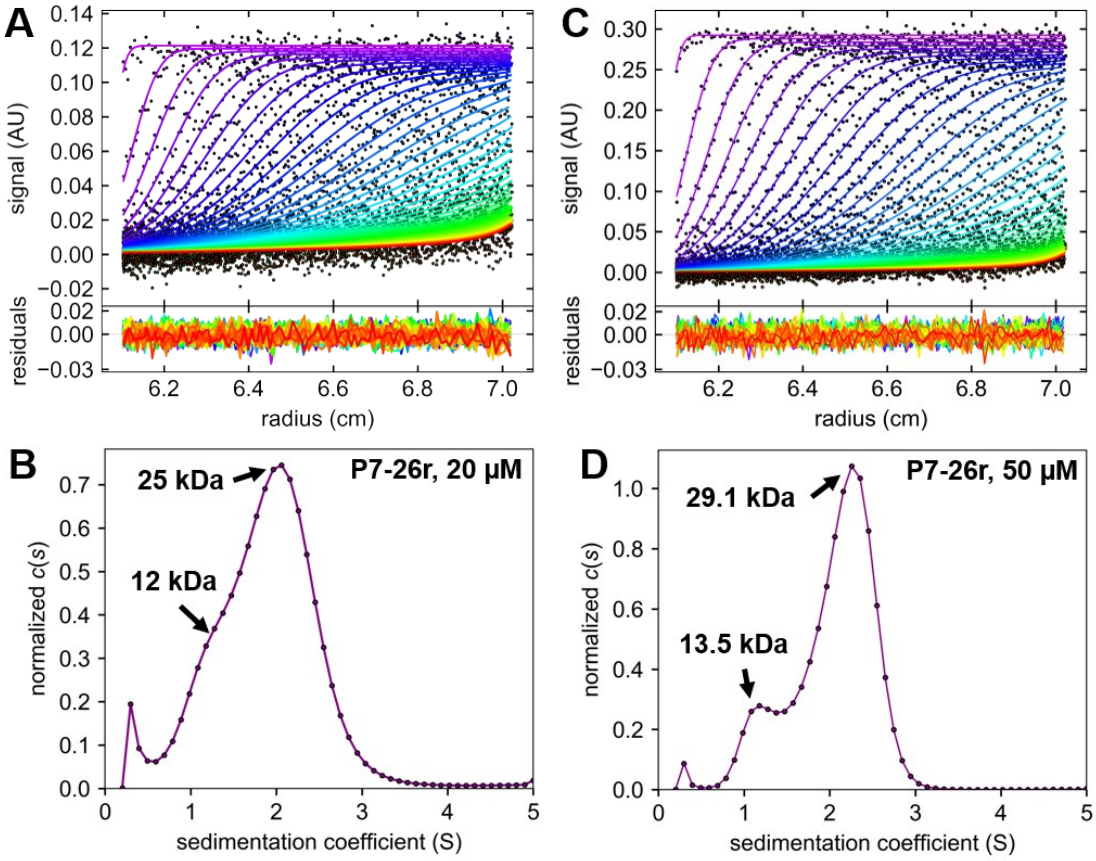

Figure S4. Analytical ultracentrifugation-sedimentation velocity (AUC-SV) experiments. Raw sedimentation profiles of absorbance at 280 nm versus cell radius for (**A**) 20 μM and (**C**) 50 μM of P7-26r and residual plot supplied by SEDFIT software showing the fitting goodness. Continuous sedimentation coefficient distribution, c(s) curve, obtained with a regularization procedure from data shown in left with a confidence level of 0.95 using SEDFIT software for (**B**) 20 μM and (**D**) 50 μM of P7-26r. The partial specific volume (v), buffer density and viscosity at room temperature were determined to be 0.73317 mL/g, 0.99914 g/mL and 0.01005 cP, respectively through SEDENTERP software.

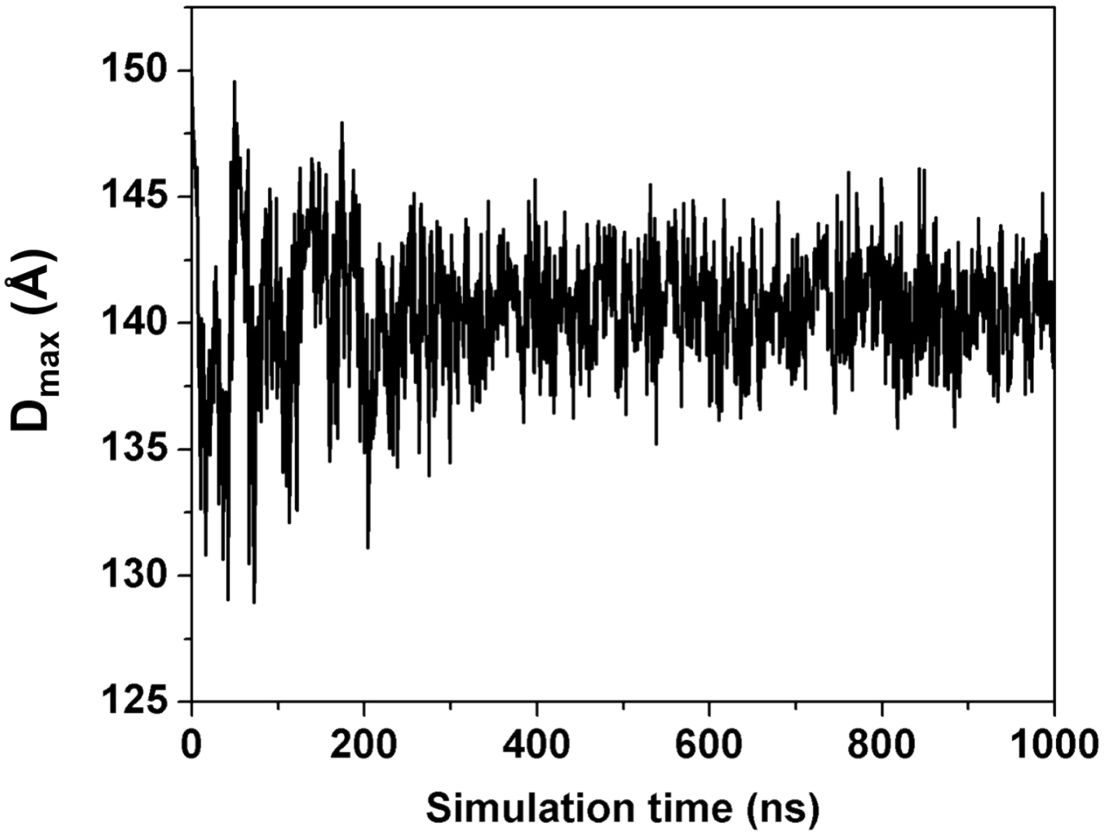

Figure S5. Maximum atom-to-atom distance of P7-26r assembly in the MD trajectory.

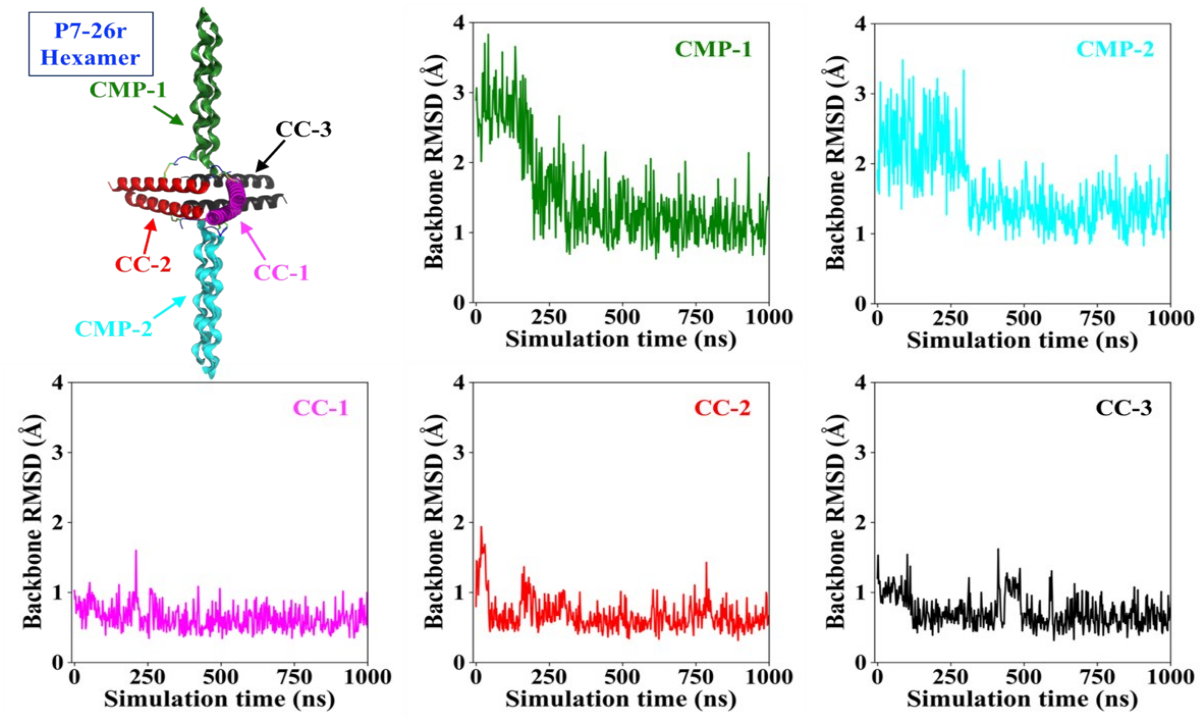

Figure S6. Root mean square deviation of the backbone atoms (C, N, Cα) developed by different domains during the simulation. The RMSD value was calculated by using the structure averaged from frames between 500 ns and 1000 ns as the reference.

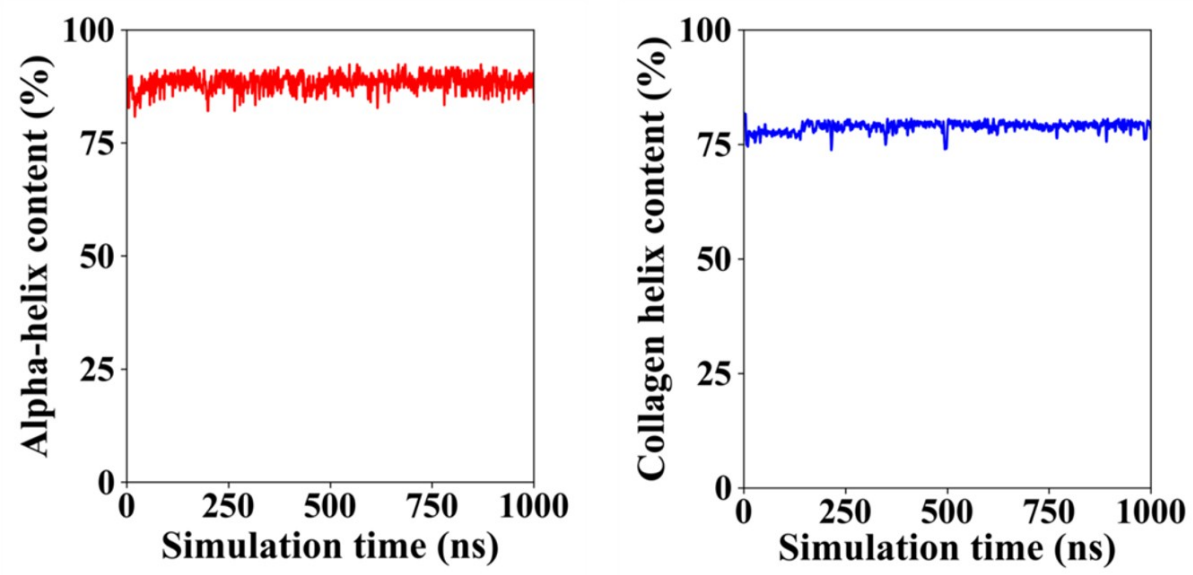

Figure S7. Content of α-helix and collagen triple helix possessed by P7-26r hexamer over the course of the simulation.

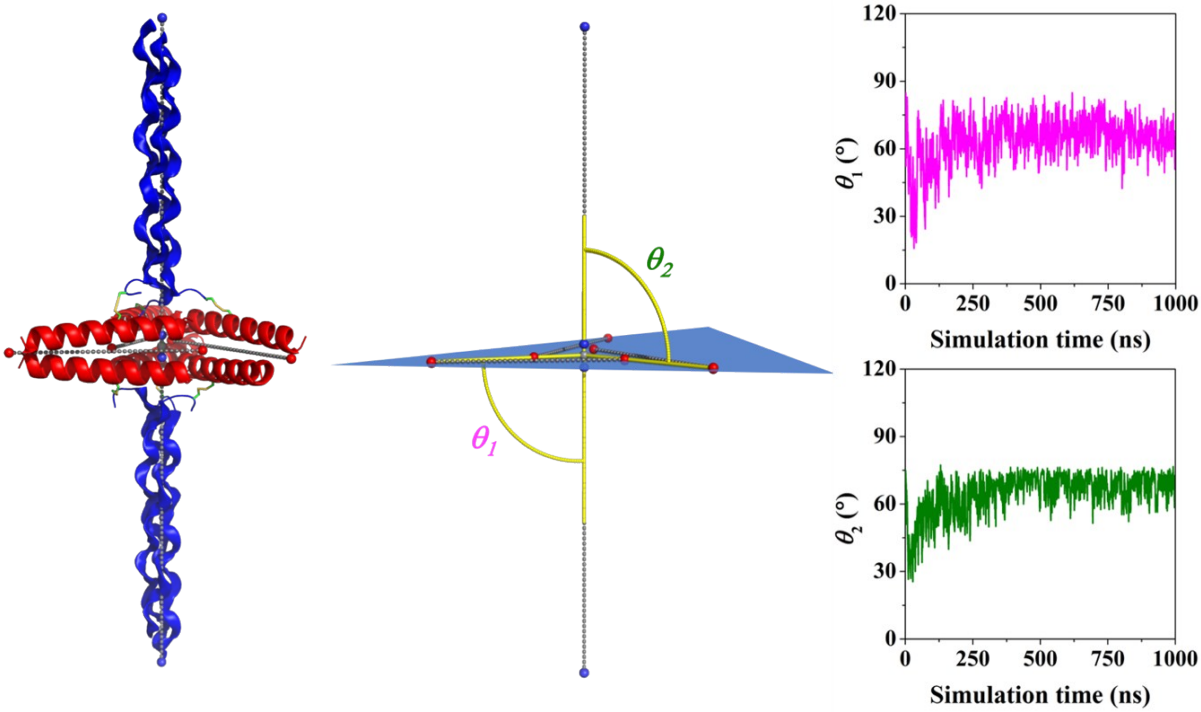

Figure S8. Analysis of the angles, θ_1 and θ_2, between the symmetry axis of collagen triple helices and the plane occupied by three coiled coil domains. Regression plane of the symmetry-axis of three coiled coil domains was used for the calculation.

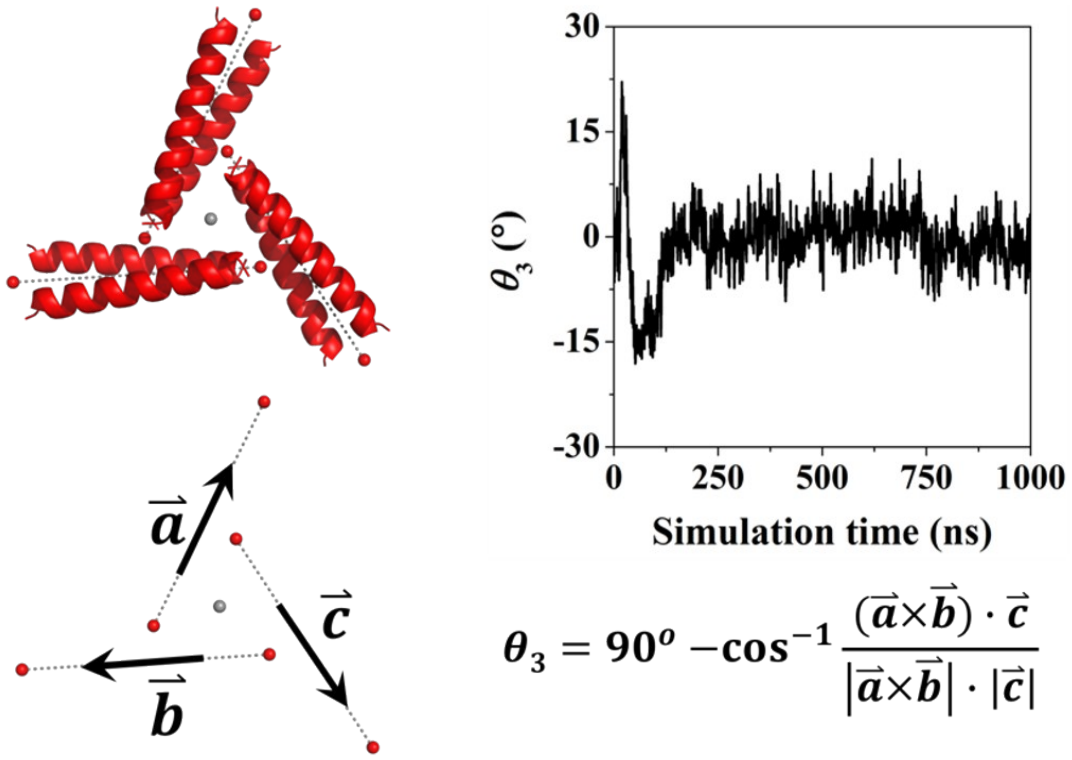

Figure S9. Analysis of the geometrical relationship of the symmetry-axis of three coiled coil domains. The three symmetry-axis are represented by three vectors, $\vec{a}$, $\vec{b}$ and $\vec{c}$. The angle, θ_3, between vector $\vec{c}$ and the plane occupied by $\vec{a}$ and $\vec{b}$ is used to estimate if the three coiled coil domains located on the same plane. A close-to-zero value indicates the three coiled coil dimers are on the same plane.

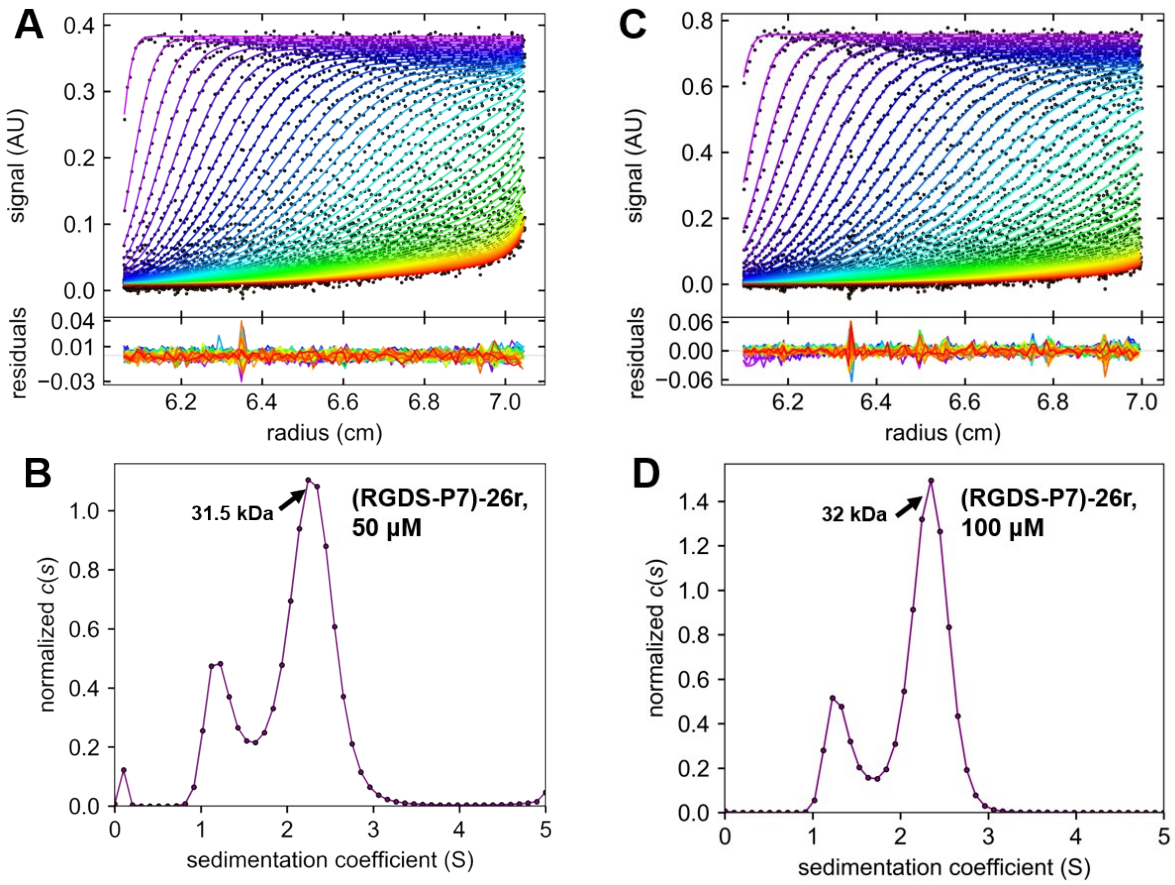

Figure S10. Sedimentation velocity analytical ultracentrifugation experiment. Raw sedimentation profiles of absorbance at 280 nm versus cell radius for (**A**) 50 µM and (**C**) 100 µM of (RGDS-P7)-26r and residual plot supplied by SEDFIT software showing the fitting goodness. Continuous sedimentation coefficient distribution, c(s) curve, obtained with a regularization procedure from data shown in left with a confidence level of 0.95 using SEDFIT software for (**B**) 50 µM and (**D**) 100 µM of (RGDS-P7)-26r. The partial specific volume (v), buffer density and viscosity at room temperature were determined to be 0.72508 mL/g, 0.99914 g/mL and 0.01005 cP, respectively through SEDENTERP software.

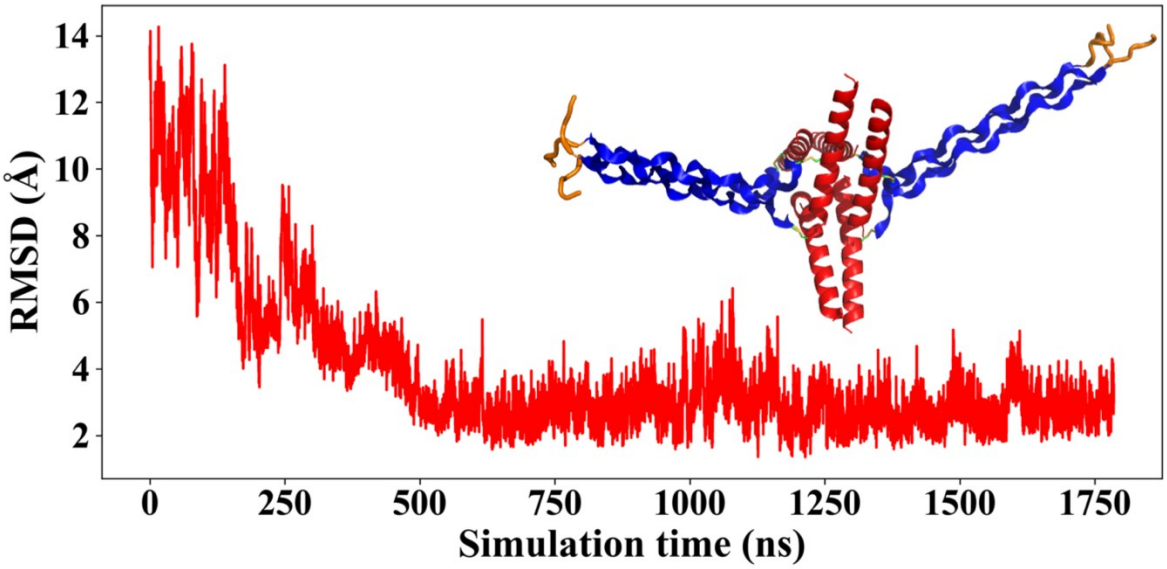

Figure S11. Root mean square deviation of the backbone atoms (C, N, Cα) of the (RGDS-P7)-26r hexamer over the course of simulation. The inset shows the coordinates averaged structure by using frames in the last 1000 ns trajectories. RMSD values were calculated by using the averaged structure as the reference. Color code for the cartoon representation, blue: P7 collagen triple helices; red: 26r coiled coil dimers; orange: RGDS ligands.

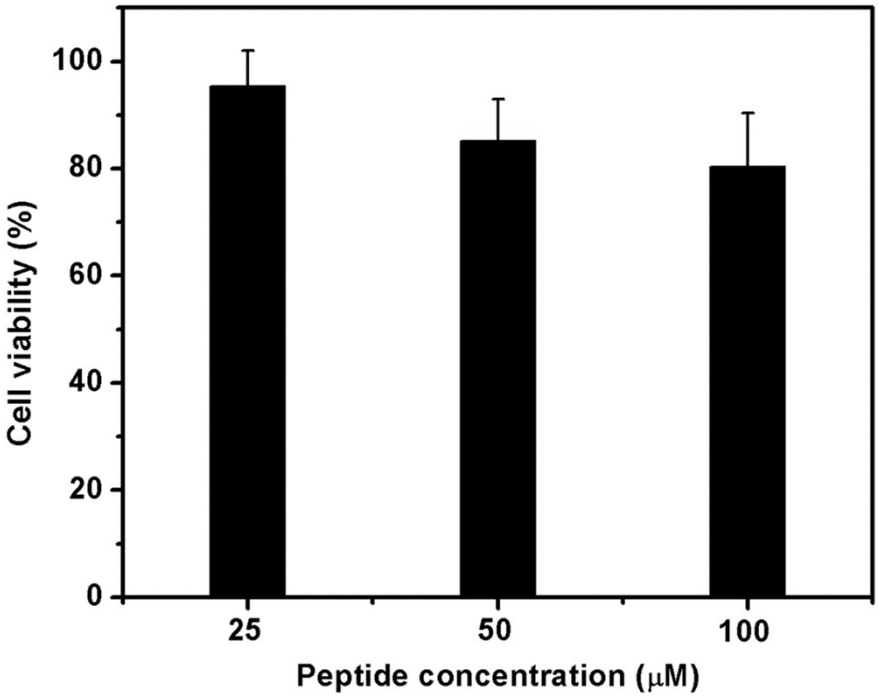

Figure S12. Cytotoxicity of (RGDS-P7)-26r assembly towards U87MG cells. The cell viability maintained at ~85% at a peptide concentration up to 100 μM, which demonstrated that (RGDS-P7)-26r assembly had very low cytotoxicity. Incubation time: 24 hrs.

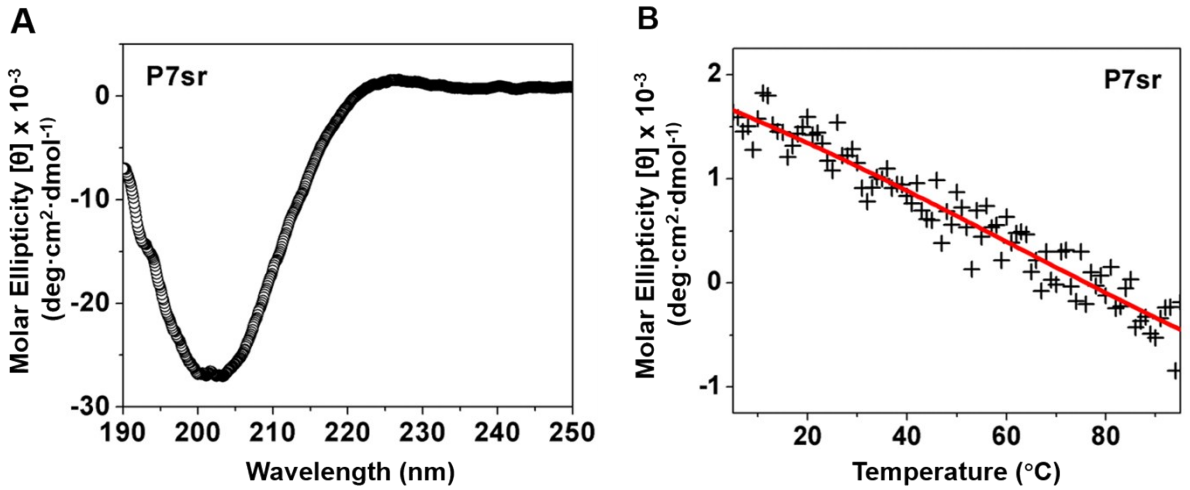

Figure S13. (**A**) CD spectrum of P7sr at 25 ℃. (**B**) Thermal unfolding profile of P7sr by monitoring the ellipticity at 225 nm. Peptide concentration: 100 μM. Buffer: 10 mM sodium phosphate buffer (pH=7.4)

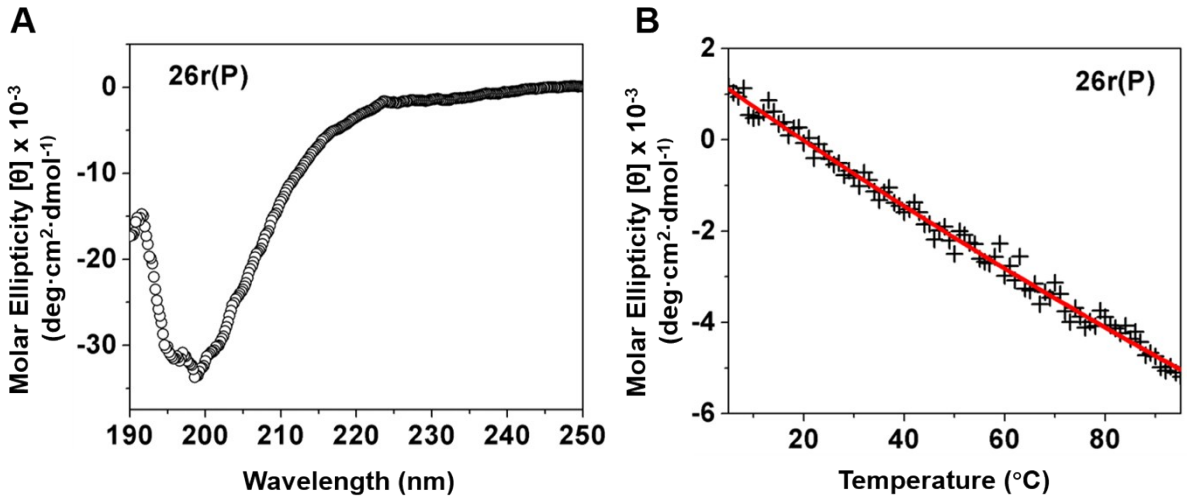

Figure S14. (**A**) CD spectrum of 26r(P) at 25 ℃. (**B**) Thermal unfolding profile of 26r(P) by monitoring the ellipticity at 225 nm. Peptide concentration: 100 μM. Buffer: 10 mM sodium phosphate buffer (pH=7.4)

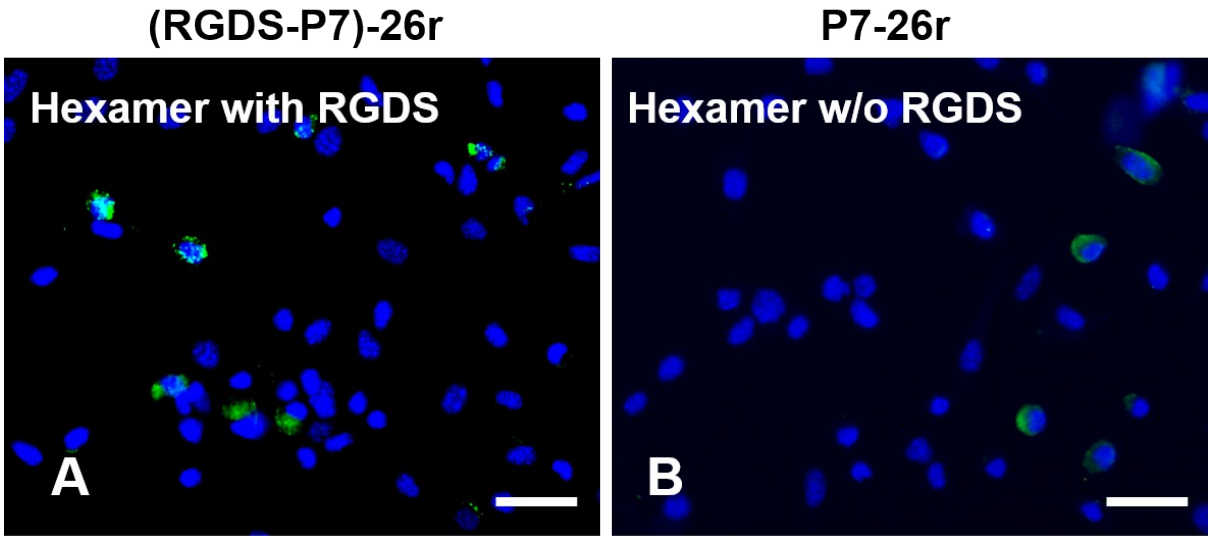

Figure S15. Fluorescence images of NIH/3T3 mouse fibroblasts treated with FITC labeled peptides. (**A**) (RGDS-P7)-26r (**hexamer**), (**B**) P7-26r (**hexamer w/o RGDS**). Incubation time: 24 hrs. Peptide concentration: 50 μM. Scale bar: 100 μm. Green: FITC labeled peptides. Blue: Hoechst 33342 nucleus staining.

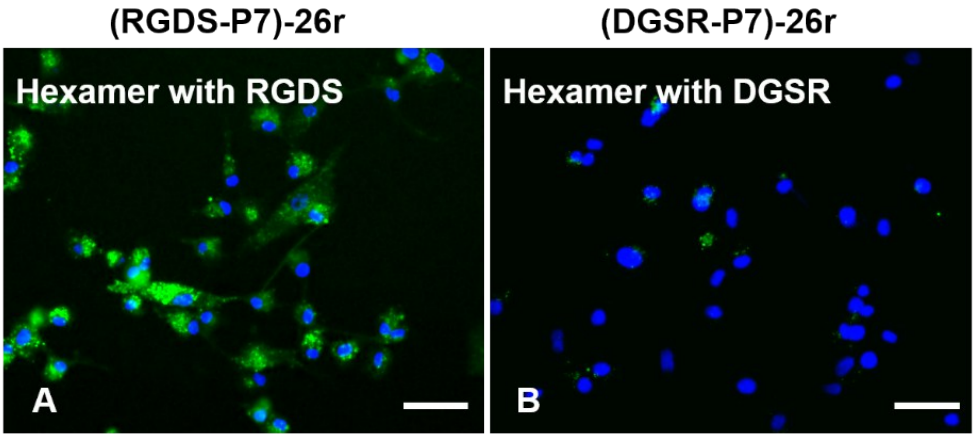

Figure S16. Fluorescence images of U87MG cells treated with FITC labeled (**A**) (RGDS-P7)-26r and (**B**) (DGSR-P7)-26r. Incubation time: 24 hrs. Peptide concentration: 50 μM. Scale bar: 100 μm. Green: FITC labeled peptides. Blue: Hoechst 33342 staining.

References

1. a) W. Liu, G. Hao, M. A. Long, T. Anthony, J.-T. Hsieh and X. Sun, *Angew. Chem. Int. Ed.*, 2009, **48**, 7346-7349; b) A. N. Singh, W. Liu, G. Hao, A. Kumar, A. Gupta, O. K. Öz, J.-T. Hsieh and X. Sun, *Bioconjug Chem*, 2011, **22**, 1650-1662; c) A. N. Singh, M. Dakanali, G. Hao, S. Ramezani, A. Kumar and X. Sun, *Eur. J. Med. Chem.*, 2014, **80**, 308-315; d) A. Kumar, S. Zhang, G. Hao, G. Hassan, S. Ramezani, K. Sagiyama, S.-T. Lo, M. Takahashi, A. D. Sherry, O. K. Öz, Z. Kovacs and X. Sun, *Bioconjug Chem*, 2015, **26**, 549-558.
2. C. D. Putnam, M. Hammel, G. L. Hura and J. A. Tainer, *Q. Rev. Biophys.*, 2007, **40**, 191-285.
3. R. P. Rambo and J. A. Tainer, *Nature*, 2013, **496**, 477-481.
4. a) P. Schuck, *Biophys. J.*, 2000, **78**, 1606-1619; b) P. Schuck, M. A. Perugini, N. R. Gonzales, G. J. Howlett and D. Schubert, *Biophys. J.*, 2002, **82**, 1096-1111.
5. T. Laue, *Curr Protoc Protein Sci*, 1999, **18**, 20.23.21-20.23.13.
6. P. Schuck and B. Demeler, *Biophys. J.*, 1999, **76**, 2288-2296.
7. C. A. Brautigam, in *Methods in Enzymology*, ed. J. L. Cole, Academic Press, 2015, vol. 562, pp. 109-133.
8. C. W. Wood and D. N. Woolfson, *Protein Sci*, 2018, **27**, 103-111.
9. R. Berisio, L. Vitagliano, L. Mazzarella and A. Zagari, *Protein Sci*, 2002, **11**, 262-270.
10. B. Ciani, S. Bjelić, S. Honnappa, H. Jawhari, R. Jaussi, A. Payapilly, T. Jowitt, M. O. Steinmetz and R. A. Kammerer, *Proc. Natl. Acad. Sci. U.S.A.*, 2010, **107**, 19850.
11. a) L. Jiang, D. Xu, K. E. Namitz, M. S. Cosgrove, R. Lund and H. Dong, *Small*, 2016, **12**, 5126-5131; b) L. Jiang, S. Yang, R. Lund and H. Dong, *Biomater Sci*, 2018, **6**, 272-279.
12. a) I. Y. B.-S. D.A. Case, S.R. Brozell, D.S. Cerutti, T.E. Cheatham, III, V.W.D. Cruzeiro, T.A. Darden,, D. G. R.E. Duke, M.K. Gilson, H. Gohlke, A.W. Goetz, D. Greene, R Harris, N. Homeyer, Y. Huang,, A. K. S. Izadi, T. Kurtzman, T.S. Lee, S. LeGrand, P. Li, C. Lin, J. Liu, T. Luchko, R. Luo, D.J., K. M. M. Mermelstein, Y. Miao, G. Monard, C. Nguyen, H. Nguyen, I. Omelyan, A. Onufriev, F. Pan, R. and D. R. R. Qi, A. Roitberg, C. Sagui, S. Schott-Verdugo, J. Shen, C.L. Simmerling, J. Smith, R. SalomonFerrer, J. Swails, R.C. Walker, J. Wang, H. Wei, R.M. Wolf, X. Wu, L. Xiao, D.M. York and P.A. Kollman, *Amber 2018*, University of California, San Francisco, 2018; b) R. Salomon-Ferrer, A. W. Gotz, D. Poole, S. Le Grand and R. C. Walker, *J Chem Theory Comput*, 2013, **9**, 3878-3888.
13. J. A. Maier, C. Martinez, K. Kasavajhala, L. Wickstrom, K. E. Hauser and C. Simmerling, *J Chem Theory Comput*, 2015, **11**, 3696-3713.
14. W. L. Jorgensen, J. Chandrasekhar, J. D. Madura, R. W. Impey and M. L. Klein, *J. Chem. Phys.*, 1983, **79**, 926-935.
15. P. Li, L. F. Song and K. M. Merz, *J Chem Theory Comput*, 2015, **11**, 1645-1657.
16. J.-P. Ryckaert, G. Ciccotti and H. J. C. Berendsen, *J. Comput. Phys.*, 1977, **23**, 327-341.
17. U. Essmann, L. Perera, M. L. Berkowitz, T. Darden, H. Lee and L. G. Pedersen, *J. Chem. Phys.*, 1995, **103**, 8577-8593.
18. J. A. Izaguirre, D. P. Catarello, J. M. Wozniak and R. D. Skeel, *J. Chem. Phys.*, 2001, **114**, 2090-2098.
19. H. J. C. Berendsen, J. P. M. Postma, W. F. van Gunsteren, A. DiNola and J. R. Haak, *J. Chem. Phys.*, 1984, **81**, 3684-3690.
20. D. R. Roe and T. E. Cheatham, *J Chem Theory Comput*, 2013, **9**, 3084-3095.